Analog and Digital Self-interference Cancellation in Full-Duplex MIMO-OFDM Transceivers with Limited Resolution in A/D Conversion

Taneli Riihonen and Risto Wichman
SMARAD Centre of Excellence and Department of Signal Processing and Acoustics
Aalto University School of Electrical Engineering, P.O. Box 13000, FI-00076 Aalto, Helsinki, Finland
Email: {taneli.riihonen, risto.wichman}@aalto.fi

***Abstract*—We analyze the performance of full-duplex MIMO-OFDM transceivers with subtractive self-interference cancellation in analog and/or digital domain, i.e., before and/or after analog-to-digital converters (ADCs). In particular, the non-ideal ADCs are modeled by assuming uniform b-bit quantization which allows us to derive closed-form expressions for the signal to interference and noise ratio when including the effects of the residual self-interference due to imperfect cancellation and the clipping-plus-quantization noise due to the limited dynamic range of ADCs. Consequently, this facilitates a study on the fundamental trade-off between ADC resolution, maximum transmit power, minimum physical isolation and sufficient signal to self-interference ratio needed to avoid receiver saturation. We also highlight the benefit of combining analog and digital cancellation: if the former attenuates interference sufficiently well such that all received signals fit within the limited dynamic range of ADCs, the latter can handle the residual self-interference efficiently.**

I. Introduction

Full-duplex wireless [1]–[9] is a progressive frequency-reuse concept, which may become reality in such scenarios as simultaneous down- and uplink transmission [8], multihop relay links [10], [11], and bidirectional links [12]. A full-duplex transceiver may transmit data to another node while simultaneously receiving its own signal of interest on the same channel, ideally rendering double spectral efficiency w.r.t. conventional systems. However, such gain is available only at the price of a significant technical issue: self-interference.

Although single-array full-duplex transceivers are envisioned to be viable in the future, current technology requires the use of separated transmit and receive arrays to obtain preliminary physical isolation. Many experiments on such transceivers and antennas are reported recently, e.g., see [13], [14]. For additional isolation, various digital self-interference mitigation schemes are necessary [15]–[17] and power control allows to balance the residual interference situation [18].

The self-interference can be at much higher level than the signal of interest while digital signal processing schemes are useless if the receiver is saturated, i.e., the desired signal is drowned in the self-interference signal. Limited dynamic range manifests itself in the form of clipping-plus-quantization noise, as modelled before [7], [15], but here studied in terms of ADC resolution following the framework of [19] for OFDM signals. In particular, we see that effective analog pre-cancellation is an essential prerequisite for the use of digital mitigation.

II. System Model

Let us consider the generic full-duplex MIMO-OFDM transceiver illustrated in Fig. 1. The device is equipped with N_r receive antennas and N_t transmit antennas that are deployed as two spatially-separated arrays to yield some preliminary physical isolation before cancellation. In contrast to many recent works on full-duplex communication, *the novel aspect herein is* not only *to account for the self-interference* but also *to model explicitly the limited dynamic range of ADCs*, which is the key factor to cause the risk of receiver saturation.

A. Signal Model at Transmitter Side

As outlined in the introduction, typical full-duplex communication scenarios involve a distant transmitter from whom the full-duplex transceiver aims to receive the signal of interest while causing self-interference by simultaneously transmitting digital signal $\mathbf{x}_\mathrm{d}[i]$ to its designated destination. The digital-to-analog converters (DACs) at the transmit side are now assumed to be ideal such that the signal after DAC is $\mathbf{x}_\mathrm{a}[i] \simeq \mathbf{x}_\mathrm{d}[i]$. Thus, the transmitted self-interference signal is denoted by $\mathbf{x}[i] \in \mathbb{C}^{N_\mathrm{t}\times 1}$ hereafter in both analog and digital domain.

B. Signal Model at Receiver Side

During the ith sampling instant, the full-duplex transceiver receives not only the signal of interest $\hat{\mathbf{y}}_\mathrm{a}[i] \in \mathbb{C}^{N_\mathrm{r}\times 1}$ but also a self-interference signal $\mathbf{z}_\mathrm{a}[i] \in \mathbb{C}^{N_\mathrm{r}\times 1}$ due to coupling between its arrays. Let us denote the MIMO impulse response of the multipath self-interference channel by $\mathbf{H}[k] \in \mathbb{C}^{N_\mathrm{r}\times N_\mathrm{t}}$, with $k = 0, 1, \ldots$ being the delay index. Consequently, the received analog composite signal to be decoded can be expressed as

$$\mathbf{y}_\mathrm{a}[i] = \hat{\mathbf{y}}_\mathrm{a}[i] + \mathbf{z}_\mathrm{a}[i] \tag{1}$$

for which discrete convolution yields

$$\mathbf{z}_\mathrm{a}[i] = \textstyle\sum_{k=0}^{\infty} \mathbf{H}[k]\,\mathbf{x}[i-k]. \tag{2}$$

Throughout the paper, we concentrate on the effects caused by the limited dynamic range of the ADCs at the receiver side while the channel impulse response $\mathbf{H}[k]$ is assumed to be known perfectly and remain constant during the transmission of each OFDM symbol. Furthermore, we focus on practical situations where the performance is limited by the self-interference and the dynamic range of the ADCs such that inherent thermal noise can be omitted in the signal models.

978-1-4673-5051-8/12/$31.00 ©2012 IEEE

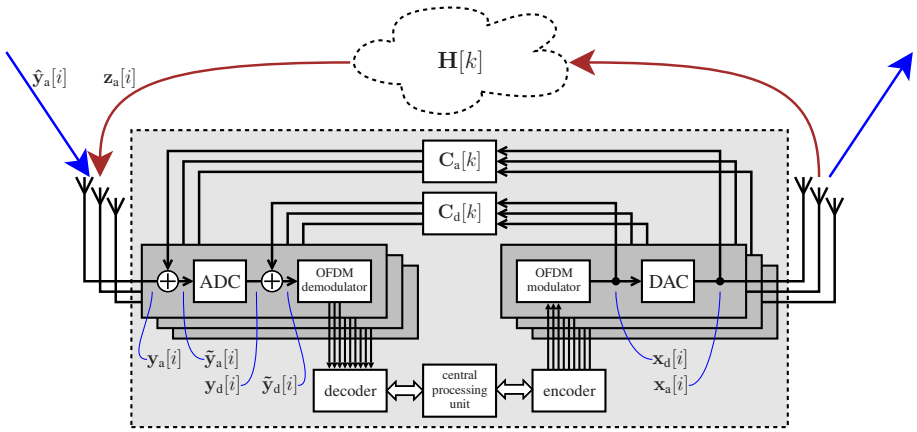

Fig. 1. Signal model for a full-duplex MIMO-OFDM transceiver with analog and digital self-interference cancellation.

1) Analog Cancellation: The principle of subtractive self-interference cancellation is to process the known transmitted signal with a frequency-selective filter to generate a negative that, when added to the composite signal, reverts the effect of the self-interference propagating through $\mathbf{H}[k]$. Denoting the impulse response of the cancellation filter by $\mathbf{C}_\mathrm{a}[k] \in \mathbb{C}^{N_\mathrm{r} \times N_\mathrm{t}}$, the input-output relation of analog cancellation becomes

$$\tilde{\mathbf{y}}_\mathrm{a}[i] = \mathbf{y}_\mathrm{a}[i] + \textstyle\sum_{k=0}^{\infty} \mathbf{C}_\mathrm{a}[k]\, \mathbf{x}[i-k] = \hat{\mathbf{y}}_\mathrm{a}[i] + \tilde{\mathbf{z}}_\mathrm{a}[i], \tag{3}$$

where the residual self-interference signal is given by

$$\tilde{\mathbf{z}}_\mathrm{a}[i] = \textstyle\sum_{k=0}^{\infty} \tilde{\mathbf{H}}_\mathrm{a}[k]\, \mathbf{x}[i-k] \tag{4}$$

and the residual loopback channel is denoted by

$$\tilde{\mathbf{H}}_\mathrm{a}[k] = \mathbf{H}[k] + \mathbf{C}_\mathrm{a}[k]. \tag{5}$$

The self-interference could be ideally removed already in analog domain by choosing $\mathbf{C}_\mathrm{a}[k] = -\mathbf{H}[k]$ for all k, which guarantees $\tilde{\mathbf{H}}_\mathrm{a}[k] = \mathbf{0}$. However, $\mathbf{C}_\mathrm{a}[k]$ is an analog filter which is difficult and expensive to implement, not least because it should be adapted according to channel fluctuations in a mobile environment. For example, a practical implementation may include only an $N_\mathrm{r} \times N_\mathrm{t}$ matrix of amplification and phase shift operations which can cancel at its best the strongest multipath component of each MIMO branch as follows:

$$\{\mathbf{C}_\mathrm{a}[k]\}_{m,n} = \begin{cases} -\{\mathbf{H}[k]\}_{m,n}, & \text{if } k = k^*_{m,n}, \\ 0, & \text{otherwise,} \end{cases} \tag{6}$$

where $k^*_{m,n} = \arg\max_k |\{\mathbf{H}[k]\}_{m,n}|^2$. Without analog cancellation, we set simply $\mathbf{C}_\mathrm{a}[k] = \mathbf{0}$ for all k which yields $\tilde{\mathbf{z}}_\mathrm{a}[i] = \mathbf{z}_\mathrm{a}[i]$ and $\tilde{\mathbf{y}}_\mathrm{a}[i] = \mathbf{y}_\mathrm{a}[i] = \hat{\mathbf{y}}_\mathrm{a}[i] + \mathbf{z}_\mathrm{a}[i]$.

2) Analog-to-Digital Conversion: At the mth antenna, the ADC processes the in-phase signal according to

$$\mathrm{Re}(\{\mathbf{y}_\mathrm{d}[i]\}_m) = \mathcal{Q}(\sqrt{g_m}\, \mathrm{Re}(\{\tilde{\mathbf{y}}_\mathrm{a}[i]\}_m)), \tag{7}$$

and similarly in the quadrature branch with $\mathrm{Im}(\cdot)$. Above g_m is the gain of the variable gain amplifier (VGA) which is tuned by automatic gain control (AGC) for maintaining signal level within the fixed scale of the quantization block $\mathcal{Q}(\cdot)$. In particular, we assume uniform b-bit ADCs with $Q = 2^b$ equidistant quantization levels, given by $y_q = 2 \cdot \frac{q-1}{Q-1} - 1$, including the respective lowest and highest signal values $y_1 = -1$ and $y_Q = 1$. Thus, the quantization block becomes

$$\mathcal{Q}(y) = \begin{cases} 1, & \text{if } \frac{Q-2}{Q-1} < y, \\ y_q, & \text{if } y_q - \frac{1}{Q-1} < y \le y_q + \frac{1}{Q-1}, \\ -1, & \text{if } y \le \frac{2-Q}{Q-1}. \end{cases} \tag{8}$$

Let us assume the transmission of OFDM signals, which are very closely Gaussian due to the central limit theorem if the number of subcarriers is large [20]. Thus, the theory of non-linear memoryless devices [21] allows to rewrite (7) as

$$\mathbf{y}_\mathrm{d}[i] = \mathbf{A}\tilde{\mathbf{y}}_\mathrm{a}[i] + \mathbf{n}[i], \tag{9}$$

where $\mathbf{A}$ is a real diagonal matrix and the clipping-plus-quantization noise term $\mathbf{n}[i]$ is uncorrelated with $\tilde{\mathbf{y}}_\mathrm{a}[i]$. Consequently, we may denote $\hat{\mathbf{y}}_\mathrm{d}[i] = \mathbf{A}\hat{\mathbf{y}}_\mathrm{a}[i]$ and $\mathbf{z}_\mathrm{d}[i] = \mathbf{A}\tilde{\mathbf{z}}_\mathrm{a}[i]$.

3) Digital Cancellation: Denoting the impulse response of the cancellation filter by $\mathbf{C}_\mathrm{d}[k] \in \mathbb{C}^{N_\mathrm{r} \times N_\mathrm{t}}$, the input-output relation of digital cancellation can be written as

$$\begin{aligned} \tilde{\mathbf{y}}_\mathrm{d}[i] &= \mathbf{y}_\mathrm{d}[i] + \textstyle\sum_{k=0}^{\infty} \mathbf{C}_\mathrm{d}[k]\, \mathbf{x}[i-k] \\ &= \hat{\mathbf{y}}_\mathrm{d}[i] + \tilde{\mathbf{z}}_\mathrm{d}[i] + \mathbf{n}[i], \end{aligned} \tag{10}$$

where the residual self-interference signal is given by

$$\tilde{\mathbf{z}}_\mathrm{d}[i] = \textstyle\sum_{k=0}^{\infty} \tilde{\mathbf{H}}_\mathrm{d}[k]\, \mathbf{x}[i-k] \tag{11}$$

and the residual loopback channel is denoted by

$$\tilde{\mathbf{H}}_\mathrm{d}[k] = \mathbf{A}\tilde{\mathbf{H}}_\mathrm{a}[k] + \mathbf{C}_\mathrm{d}[k]. \tag{12}$$

The self-interference could be removed now by choosing

$$\mathbf{C}_\mathrm{d}[k] = -\mathbf{A}\tilde{\mathbf{H}}_\mathrm{a}[k] = -\mathbf{A}(\mathbf{H}[k] + \mathbf{C}_\mathrm{a}[k]) \tag{13}$$

for all k, which guarantees $\tilde{\mathbf{H}}_\mathrm{d}[k] = \mathbf{0}$. Unfortunately, digital cancellation cannot suppress the noise term $\mathbf{n}[i]$ induced for the most part by the residual self-interference remaining after analog cancellation. Moreover, some interference will leak also through a residual channel due to channel estimation errors. Without digital cancellation, we set simply $\mathbf{C}_\mathrm{d}[k] = \mathbf{0}$ for all k which yields $\tilde{\mathbf{z}}_\mathrm{d}[i] = \mathbf{z}_\mathrm{d}[i] = \mathbf{A}\tilde{\mathbf{z}}_\mathrm{a}[i]$ and $\tilde{\mathbf{y}}_\mathrm{d}[i] = \mathbf{y}_\mathrm{d}[i]$.

$$\rho = \left[2\pi \frac{2\,\Phi\left(\frac{1}{\sqrt{p}}\frac{2-Q}{Q-1}\right) + \sum_{q=2}^{Q-1}\left(\frac{2q-2}{Q-1}-1\right)^2\left[\Phi\left(\frac{1}{\sqrt{p}}\left(\frac{2q-1}{Q-1}-1\right)\right) - \Phi\left(\frac{1}{\sqrt{p}}\left(\frac{2q-3}{Q-1}-1\right)\right)\right]}{\left(2\,e^{-\frac{1}{2p}\left(\frac{2-Q}{Q-1}\right)^2} + \sum_{q=2}^{Q-1}\left(\frac{2q-2}{Q-1}-1\right)\left[e^{-\frac{1}{2p}\left(\frac{2q-3}{Q-1}-1\right)^2} - e^{-\frac{1}{2p}\left(\frac{2q-1}{Q-1}-1\right)^2}\right]\right)^2} - 1 \right]^{-1} \tag{27}$$

III. SINR Analysis

Aiming at compressed notation by omitting the time and antenna indices, let us define the respective signal, interference and noise powers at the mth receive antenna as follows:

$$P_{\mathrm{S}} = \mathcal{E}\{|\{\hat{\mathbf{y}}_{\mathrm{a}}[i]\}_m|^2\}, \tag{16}$$

$$P_{\mathrm{I}} = \mathcal{E}\{|\{\mathbf{z}_{\mathrm{a}}[i]\}_m|^2\}, \tag{17}$$

$$P_{\mathrm{N}} = \mathcal{E}\{|\{\mathbf{n}[i]\}_m|^2\}. \tag{18}$$

For the same purpose, ADC amplification factor is denoted by $\alpha = \{\mathbf{A}\}_{m,m}$, and the respective interference suppression levels due to analog and digital cancellation are defined as

$$\Delta_{\mathrm{a}} = \frac{\mathcal{E}\{|\{\mathbf{z}_{\mathrm{a}}[i]\}_m|^2\}}{\mathcal{E}\{|\{\tilde{\mathbf{z}}_{\mathrm{a}}[i]\}_m|^2\}} = \frac{P_{\mathrm{I}}}{\mathcal{E}\{|\{\tilde{\mathbf{z}}_{\mathrm{a}}[i]\}_m|^2\}}, \tag{19}$$

$$\Delta_{\mathrm{d}} = \frac{\mathcal{E}\{|\{\mathbf{z}_{\mathrm{d}}[i]\}_m|^2\}}{\mathcal{E}\{|\{\tilde{\mathbf{z}}_{\mathrm{d}}[i]\}_m|^2\}} = \frac{\alpha^2\mathcal{E}\{|\{\tilde{\mathbf{z}}_{\mathrm{a}}[i]\}_m|^2\}}{\mathcal{E}\{|\{\tilde{\mathbf{z}}_{\mathrm{d}}[i]\}_m|^2\}}. \tag{20}$$

At the mth receive antenna, the ADC output power is calculated from (9) as

$$\mathcal{E}\{|\{\mathbf{y}_{\mathrm{d}}[i]\}_m|^2\} = \alpha^2\mathcal{E}\{|\{\tilde{\mathbf{y}}_{\mathrm{a}}[i]\}_m|^2\} + P_{\mathrm{N}} \tag{21}$$

for which ADC input power can be calculated from (3) as

$$\begin{aligned}\mathcal{E}\{|\{\tilde{\mathbf{y}}_{\mathrm{a}}[i]\}_m|^2\} &= P_{\mathrm{S}} + \mathcal{E}\{|\{\tilde{\mathbf{z}}_{\mathrm{a}}[i]\}_m|^2\} \\ &= P_{\mathrm{S}} + P_{\mathrm{I}}/\Delta_{\mathrm{a}}\end{aligned} \tag{22}$$

using (19). Consequently, the dynamic range, i.e., the signal-to-quantization-plus-clipping noise ratio after ADC, becomes

$$\rho = \frac{\alpha^2\mathcal{E}\{|\{\tilde{\mathbf{y}}_{\mathrm{a}}[i]\}_m|^2\}}{P_{\mathrm{N}}} = \frac{\alpha^2(P_{\mathrm{S}} + P_{\mathrm{I}}/\Delta_{\mathrm{a}})}{P_{\mathrm{N}}}. \tag{23}$$

Since $\mathcal{E}\{|\{\hat{\mathbf{y}}_{\mathrm{d}}[i]\}_m|^2\} = \alpha^2 P_{\mathrm{S}}$, signal power after digital cancellation is calculated from (10) as

$$\mathcal{E}\{|\{\tilde{\mathbf{y}}_{\mathrm{d}}[i]\}_m|^2\} = \alpha^2 P_{\mathrm{S}} + \mathcal{E}\{|\{\tilde{\mathbf{z}}_{\mathrm{d}}[i]\}_m|^2\} + P_{\mathrm{N}} \tag{24}$$

for which we obtain

$$\mathcal{E}\{|\{\tilde{\mathbf{z}}_{\mathrm{d}}[i]\}_m|^2\} = \frac{\alpha^2 P_{\mathrm{I}}}{\Delta_{\mathrm{a}}\Delta_{\mathrm{d}}} \tag{25}$$

by combining (19) and (20). Finally, the signal-to-interference and noise ratio (SINR) can be calculated from the above expressions as

$$\gamma = \frac{\alpha^2 P_{\mathrm{S}}}{\mathcal{E}\{|\{\tilde{\mathbf{z}}_{\mathrm{d}}[i]\}_m|^2\} + P_{\mathrm{N}}} = \frac{\rho}{\frac{P_{\mathrm{S}}}{P_{\mathrm{I}}/\Delta_{\mathrm{a}}} + \rho/\Delta_{\mathrm{d}} + 1} \cdot \frac{P_{\mathrm{S}}}{P_{\mathrm{I}}/\Delta_{\mathrm{a}}} \tag{26}$$

for which dynamic range ρ is given in (23). In particular, it should be noted that this general expression is valid with any type of ADC and AGC such that their effect is seen only through ρ, and that $P_{\mathrm{S}}/(P_{\mathrm{I}}/\Delta_{\mathrm{a}})$ represents signal-to-interference ratio (SIR) after analog cancellation.

In the following, we derive dynamic range for the specific case of uniform b-bit quantization for which nonlinear input–output relation $\mathcal{Q}(\cdot)$ is defined in (8). The final result is expression (27) shown above in which $Q = 2^b$ and $\Phi(\cdot)$ denotes the standard normal cumulative distribution function.

Let us denote that the AGC drives the VGA setting g_m such that the normalized input power to the quantizer block is

$$p = \mathcal{E}\{|\sqrt{g_m}\{\tilde{\mathbf{y}}_{\mathrm{a}}[i]\}_m|^2\} = g\,(P_{\mathrm{S}} + P_{\mathrm{I}}/\Delta_{\mathrm{a}}) \tag{28}$$

where we denote $g = g_m$. This transforms the dynamic range from (23) to

$$\rho = \frac{\alpha^2 p}{g P_{\mathrm{N}}} \tag{29}$$

for which we need to evaluate α and P_{N} given b and p.

- Correlation between ADC's input and output signals can be calculated using (9) as

$$\mathcal{E}\{\{\tilde{\mathbf{y}}_{\mathrm{a}}^*[i]\}_m\{\mathbf{y}_{\mathrm{d}}[i]\}_m\} = \alpha\,\mathcal{E}\{|\{\tilde{\mathbf{y}}_{\mathrm{a}}[i]\}_m|^2\} \tag{30}$$

since $\mathcal{E}\{\{\tilde{\mathbf{y}}_{\mathrm{a}}^*[i]\}_m\{\mathbf{n}[i]\}_m\} = 0$. Consequently,

$$\alpha = \frac{g}{p}\,\mathcal{E}\{\{\tilde{\mathbf{y}}_{\mathrm{a}}^*[i]\}_m\{\mathbf{y}_{\mathrm{d}}[i]\}_m\}. \tag{31}$$

- The clipping-plus-quantization noise power can be expressed by combining (21), (22), and (28) as

$$P_{\mathrm{N}} = \mathcal{E}\{|\{\mathbf{y}_{\mathrm{d}}[i]\}_m|^2\} - \frac{p}{g}\alpha^2. \tag{32}$$

By substituting (31) and (32), (29) can be transformed to

$$\rho = \left[\frac{\mathcal{E}\{|\{\mathbf{y}_{\mathrm{d}}[i]\}_m|^2\}}{\frac{g}{p}\left(\mathcal{E}\{\{\tilde{\mathbf{y}}_{\mathrm{a}}^*[i]\}_m\{\mathbf{y}_{\mathrm{d}}[i]\}_m\}\right)^2} - 1\right]^{-1} \tag{33}$$

in which the remaining expectations [19] to be calculated are

$$\mathcal{E}\{|\{\mathbf{y}_{\mathrm{d}}[i]\}_m|^2\} = \int_{-\infty}^{\infty}[\mathcal{Q}(s)]^2 f(s)\,\mathrm{d}s, \tag{34}$$

$$\mathcal{E}\{\{\tilde{\mathbf{y}}_{\mathrm{a}}^*[i]\}_m\{\mathbf{y}_{\mathrm{d}}[i]\}_m\} = \int_{-\infty}^{\infty}\frac{s}{\sqrt{g}}\mathcal{Q}(s)f(s)\,\mathrm{d}s. \tag{35}$$

The probability density function of ADC input signal can be accurately approximated by

$$f(s) = \frac{1}{\sqrt{2\pi p}}e^{-\frac{1}{2p}s^2} \tag{36}$$

because OFDM signals become closely Gaussian due to the central limit theorem [20] if the number of subcarriers is large enough. Consequently, after substituting the piecewise constant quantization function from (8), the above integrals (34) and (35) can be solved in terms of the cumulative distribution function of the standard normal distribution

$$\Phi(x) = \frac{1}{\sqrt{2\pi}}\int_{-\infty}^{x} e^{-\frac{1}{2}s^2}ds \tag{37}$$

and the exponential function, respectively; and the final result, shown in (27), is obtained by substituting them in (33).

IV. Numerical Results

The A/D conversion affects SINR through ρ which in turn depends in the case of uniform quantization only on the number of quantization levels $Q = 2^b$, i.e., ADC resolution in bits, and the normalized input power of the quantization block, p. In particular, since SINR is monotonically increasing in terms of ρ, the system should always aim at maximizing ρ irrespective of P_{S}, P_{I}, Δ_{a} and Δ_{d} which do not affect ρ. Given fixed b, SINR is maximized when the dynamic range is

$$\rho^* = \max_p \rho \tag{38}$$

and AGC sets the normalized input power of the quantization block as $p^* = \arg\max_p \rho$. When $p < p^*$, quantization noise dominates the performance, leading to underutilization of the dynamic range offered by the available ADC resolution; and when $p > p^*$, the signal is clipped too frequently.

Figure 2 illustrates the dynamic range in terms of AGC bias, i.e., deviation from the optimal normalized input power. In general, we note that ρ^* increases and p^* decreases in terms of b. This means that higher ADC resolution allows to trade off quantization noise level for lower clipping probability, and the AGC needs to be designed taking into account the ADC resolution since constant VGA setting would inevitably result in significant AGC bias and loss of dynamic range. Actually, AGC bias may easily eat away the benefit of employing better ADC, especially if the VGA setting is too large. On the other hand, low VGA setting is a safe choice.

Linear least-squares fit for ρ^* at $b = 1, 2, \ldots, 20$ yields

$$\rho^* \simeq 5.54 \cdot b - 3.26 \text{ [dB]} \tag{39}$$

deviating from the true values at maximum 1dB which is less than the effect of AGC bias. This trend can be contrasted with the classic rule of thumb, $6.02 \cdot b + 1.76$ [dB], which is calculated by assuming that the input signal of the quantization block is a full-amplitude sine wave (no clipping) and approximating that the quantization noise follows uniform distribution. However, OFDM signal has high peak-to-average power ratio which makes the classic rule for dynamic range rather optimistic, e.g., there is about 11dB gap when $b = 12$.

Figure 3 illustrates SINR in terms of dynamic range suggesting that the performance is actually not limited at all by dynamic range if $\Delta_{\mathrm{d}} < \rho$. In the following, we assume $\rho = 60$dB as a practical example value for dynamic range, corresponding to $b = 12$-bit (resp. 14-bit) quantization with small 3dB (resp. large 14dB) loss from AGC bias, while digital suppression by more than 60dB would be rather idealistic.

Figure 4 illustrates how digital suppression improves the achieved SINR. In particular, SINR increases linearly in terms of digital suppression until performance is limited by the ADC dynamic range or imperfect analog cancellation. In fact, the SINR given in (26) is bounded by

$$\gamma \leq \min\left\{\rho, \rho \cdot \Delta_{\mathrm{a}} \frac{P_{\mathrm{S}}}{P_{\mathrm{I}}}, \Delta_{\mathrm{a}}\Delta_{\mathrm{d}} \frac{P_{\mathrm{S}}}{P_{\mathrm{I}}}\right\}. \tag{40}$$

The plot also justifies the usage of (40) as a good approximation for (26) since the curves are almost piece-wise linear.

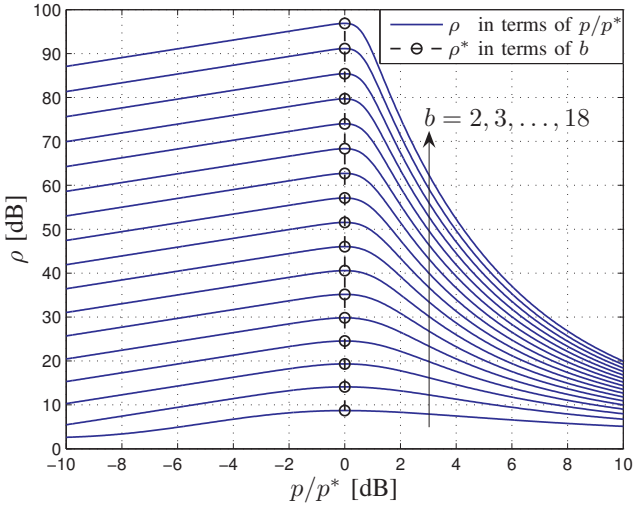

Fig. 2. Dynamic range in terms of AGC bias with different ADC resolutions.

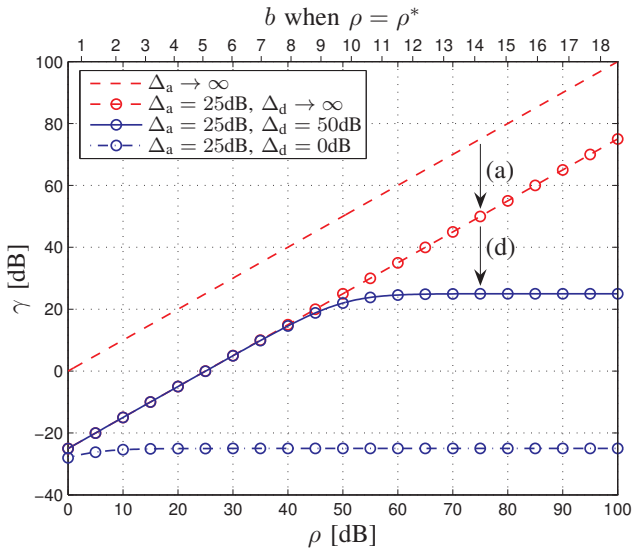

Fig. 3. Achieved SINR in terms of dynamic range when $P_{\mathrm{S}}/P_{\mathrm{I}} = -50$dB. The arrows indicate SINR loss due to (a) non-ideal analog cancellation and (d) non-ideal digital cancellation with limited ADC resolution.

Let us then assume that successful operation means the full-duplex transceiver achieves target SINR $\gamma_{\mathrm{t}} \ll \rho$. Consequently, the minimal level of digital suppression needed to guarantee $\gamma \geq \gamma_{\mathrm{t}}$ given $P_{\mathrm{S}}/P_{\mathrm{I}}$, Δ_{a} and ρ can be solved from (26) as

$$\Delta_{\mathrm{d}} \geq \frac{\rho}{\frac{P_{\mathrm{S}}}{P_{\mathrm{I}}/\Delta_{\mathrm{a}}}\left(\frac{\rho}{\gamma_{\mathrm{t}}} - 1\right) - 1} \tag{41}$$

if $\Delta_{\mathrm{a}} \frac{P_{\mathrm{S}}}{P_{\mathrm{I}}} \geq \frac{\gamma_{\mathrm{t}}}{\rho}$ or otherwise the target SINR cannot be achieved with any level of digital suppression. When $\Delta_{\mathrm{a}} \frac{P_{\mathrm{S}}}{P_{\mathrm{I}}} \gg \frac{\gamma_{\mathrm{t}}}{\rho}$, the requirement for combined digital and analog cancellation can be approximately transformed from (41) to $\Delta_{\mathrm{a}}\Delta_{\mathrm{d}} \geq \frac{\gamma_{\mathrm{t}}}{P_{\mathrm{S}}/P_{\mathrm{I}}}$. Figure 5 illustrates the combination of analog and digital suppression needed to achieve target SINR of 25dB, i.e., SIR after analog cancellation needs to be at least -35dB to make digital cancellation effective since the dynamic range is 60dB.

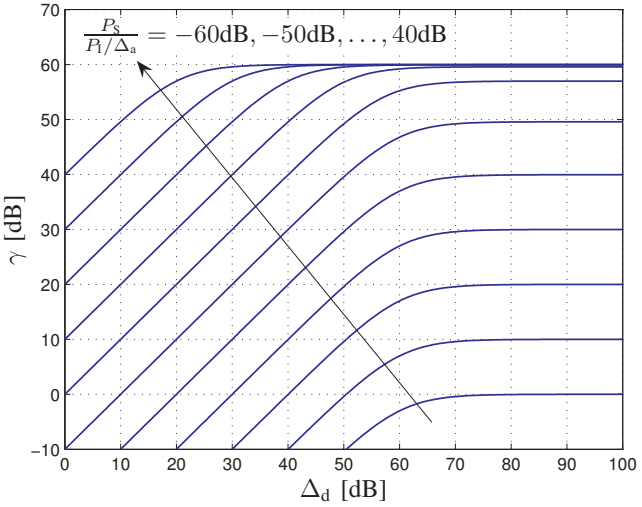

Fig. 4. Achieved SINR in terms of digital suppression with different post-analog cancellation SIRs when $\rho = 60$dB.

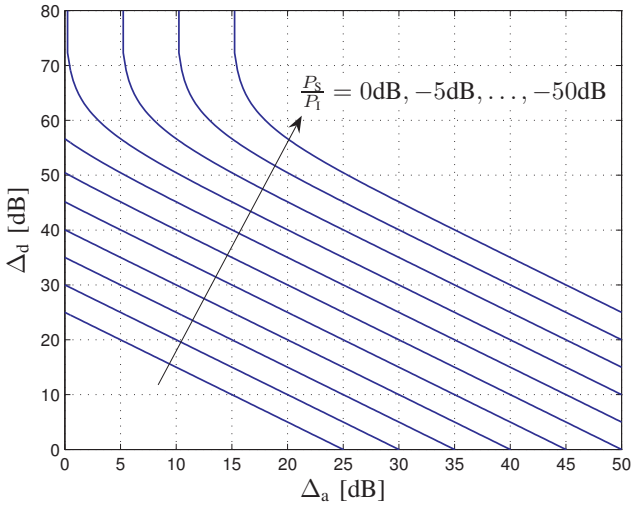

Fig. 5. Combinations of minimal analog and digital suppression required to achieve target SINR $\gamma_t = 25$dB with different input SIRs when $\rho = 60$dB.

V. Conclusions

Full-duplex receivers suffer from limited dynamic range which manifests itself in the form of clipping and quantization noise. In particular, digital interference mitigation schemes are useless if the receiver is saturated, i.e., the desired signal is drowned in the self-interference signal which can be much stronger. The non-ideal analog-to-digital conversion is here modeled explicitly by assuming uniform b-bit quantization of OFDM signals. Consequently, this facilitates a study on the fundamental trade-off between ADC resolution, sufficient signal to self-interference ratio before and after analog cancellation needed to avoid receiver saturation, and the effects of the residual self-interference due to imperfect cancellation. It seems that performance is limited more likely by the total analog and digital suppression than by the dynamic range.

References

[1] D. W. Bliss, P. A. Parker, and A. R. Margetts, "Simultaneous transmission and reception for improved wireless network performance," in *Proc. IEEE 14th Workshop on Statistical Signal Processing*, Aug. 2007.

[2] T. Riihonen, S. Werner, J. Cousseau, and R. Wichman, "Design of co-phasing allpass filters for full-duplex OFDM relays," in *Proc. 42nd Asilomar Conference on Signals, Systems, and Computers*, Oct. 2008.

[3] T. Riihonen, S. Werner, and R. Wichman, "Spatial loop interference suppression in full-duplex MIMO relays," in *Proc. 43rd Asilomar Conference on Signals, Systems, and Computers*, Nov. 2009.

[4] M. Duarte and A. Sabharwal, "Full-duplex wireless communications using off-the-shelf radios: Feasibility and first results," in *Proc. 44th Asilomar Conference on Signals, Systems, and Computers*, Nov. 2010.

[5] P. Lioliou, M. Viberg, M. Coldrey, and F. Athley, "Self-interference suppression in full-duplex MIMO relays," in *Proc. 44th Asilomar Conference on Signals, Systems, and Computers*, Nov. 2010.

[6] T. Riihonen, S. Werner, and R. Wichman, "Residual self-interference in full-duplex MIMO relays after null-space projection and cancellation," in *Proc. 44th Asilomar Conference on Signals, Systems, and Computers*, Nov. 2010.

[7] B. P. Day, D. W. Bliss, A. R. Margetts, and P. Schniter, "Full-duplex bidirectional MIMO: Achievable rates under limited dynamic range," in *Proc. 45th Asilomar Conference on Signals, Systems, and Computers*, Nov. 2011.

[8] E. Everett, M. Duarte, C. Dick, and A. Sabharwal, "Empowering full-duplex wireless communication by exploiting directional diversity," in *Proc. 45th Asilomar Conference on Signals, Systems, and Computers*, Nov. 2011.

[9] T. Riihonen, S. Werner, and R. Wichman, "Transmit power optimization for multiantenna decode-and-forward relays with loopback self-interference from full-duplex operation," in *Proc. 45th Asilomar Conference on Signals, Systems, and Computers*, Nov. 2011.

[10] B. P. Day, A. R. Margetts, D. W. Bliss, and P. Schniter, "Full-duplex MIMO relaying: Achievable rates under limited dynamic range," *IEEE Journal on Selected Areas in Communications*, vol. 30, no. 8, pp. 1541–1553, Sep. 2012.

[11] T. Riihonen, S. Werner, and R. Wichman, "Hybrid full-duplex/half-duplex relaying with transmit power adaptation," *IEEE Transactions on Wireless Communications*, vol. 10, no. 9, pp. 3074–3085, Sep. 2011.

[12] D. Senaratne and C. Tellambura, "Beamforming for space division duplexing," in *Proc. IEEE International Conference on Communications*, Jun. 2011.

[13] K. Haneda, E. Kahra, S. Wyne, C. Icheln, and P. Vainikainen, "Measurement of loop-back interference channels for outdoor-to-indoor full-duplex radio relays," in *Proc. 4th European Conference on Antennas and Propagation*, Apr. 2010.

[14] M. Duarte, C. Dick, and A. Sabharwal, "Experiment-driven characterization of full-duplex wireless systems," *IEEE Transactions on Wireless Communications*, 2012, in press.

[15] T. Riihonen, S. Werner, and R. Wichman, "Mitigation of loopback self-interference in full-duplex MIMO relays," *IEEE Transactions on Signal Processing*, vol. 59, no. 12, pp. 5983–5993, Dec. 2011.

[16] E. Everett, D. Dash, C. Dick, and A. Sabharwal, "Self-interference cancellation in multi-hop full-duplex networks via structured signaling," in *Proc. 49th Annual Allerton Conference on Communication, Control, and Computing*, Sep. 2011.

[17] T. Riihonen, A. Balakrishnan, K. Haneda, S. Wyne, S. Werner, and R. Wichman, "Optimal eigenbeamforming for suppressing self-interference in full-duplex MIMO relays," in *Proc. 45th Annual Conference on Information Sciences and Systems*, Mar. 2011.

[18] T. Riihonen, K. Haneda, S. Werner, and R. Wichman, "SINR analysis of full-duplex OFDM repeaters," in *Proc. 20th IEEE International Symposium on Personal, Indoor and Mobile Radio Communications*, Sep. 2009.

[19] D. Dardari, "Joint clip and quantization effects characterization in OFDM receivers," *IEEE Transactions on Circuits and Systems I: Regular Papers*, vol. 53, no. 8, pp. 1741–1748, Aug. 2006.

[20] S. Wei, D. L. Goeckel, and P. A. Kelly, "Convergence of the complex envelope of bandlimited OFDM signals," *IEEE Transactions on Information Theory*, vol. 56, no. 10, pp. 4893–4904, Oct. 2010.

[21] H. E. Rowe, "Memoryless nonlinearities with Gaussian inputs: Elementary results," *Bell System Technical Journal*, vol. 61, no. 7, pp. 1519–1525, Sep. 1982.